

# Upcycled waste-derived triboelectric nanogenerator for sustainable energy harvesting

Archana PANDA<sup>1</sup>, Basanta Kumar PANIGRAHI<sup>2,\*</sup>, Subhendu PATI<sup>2</sup>, Sunit Gourav MOHANTY<sup>3</sup>, and Kushal Ruthvik KAJA<sup>4,\*</sup>

## Received date:

21 July 2025

#### Revised date:

7 August 2025

#### Accepted date:

15 August 2025

#### **Keywords:**

Triboelectric nanogenerator; Sustainable energy harvesting; Neural network classifier

#### **Abstract**

The proliferation of disposable paper-based materials in laboratories has raised significant environmental concerns due to their rapid discard and accumulation. This study explores the upcycling of commonly discarded laboratory waste, specifically butter paper and polyurethane (PU) foam, into a single-electrode triboelectric nanogenerator (TENG) for mechanical energy harvesting. The fabricated device employs butter paper as the positive triboelectric layer and PU foam as the negative layer, with an aluminium tape electrode. Electrical tests reveal a peak voltage of 21 V and current of 47 nA, reaching a maximum power of 438 nW at 500 M $\Omega$  load. The TENG demonstrates stable performance over three weeks and efficiently charges capacitors of various capacitances. Its sensitivity to biomechanical stimuli such as finger, palm, and foot tapping showcases potential applications in wearable electronics and gesture recognition. Integration with a neural network classifier achieves high accuracy in input pattern recognition, underscoring the device's promise for sustainable energy harvesting and smart sensing technologies in laboratory waste valorisation.

# 1. Introduction

The continuous growth of scientific research and clinical diagnostics has led to an unprecedented accumulation of laboratory waste, raising serious environmental and sustainability concerns. Among the various categories of waste generated, paper-based materials, such as filter paper, tissue wipes, weighing paper, and butter paper, constitute a major portion due to their widespread utility in everyday experimental workflows [1-3]. These materials are frequently employed for filtration, cleaning, sample handling, and weighing procedures, owing to their affordability, sterility, and ease of use. However, their inherently disposable nature and strict single-use protocols, necessitated by the need to avoid contamination and ensure experimental reliability, result in their rapid turnover and disposal. This continuous cycle of consumption and discard not only strains waste management systems but also contributes to the broader issue of resource inefficiency and environmental degradation [4,5]. As laboratory practices increasingly demand sterile and reliable materials, a paradox emerges between operational necessity and ecological responsibility, emphasizing the urgent need for sustainable waste mitigation strategies within scientific environments [6,7].

In response to the urgent need for eco-friendly solutions, the concept of upcycling laboratory waste into functional energy devices has gained notable momentum [8-12]. Among the innovative approaches, triboelectric nanogenerators (TENGs) have emerged as a versatile technology capable of converting ambient mechanical energy into electrical energy through the triboelectric effect [13-17]. TENGs are particularly attractive due to their simple fabrication, low cost, and adaptability to a wide array of materials, including those derived from waste streams [18-22]. By integrating waste materials into TENG design, researchers address both energy harvesting and waste reduction, aligning with the principles of circular economy and sustainable development [23-26]. In a recent study, Hajra et al. demonstrated the fabrication of a TENG utilizing discarded textile materials as tribolayers, achieving an output voltage of 19 V and a current of 8  $\mu A$ [27]. Similarly, Rani and co-workers developed a TENG based on repurposed cigarette filter waste, operating in a vertical contactseparation mode, which generated an output of 42.8 V and 0.86 µA [28]. In another study, Jeong et al. engineered a TENG using cotton fabric, reporting an output performance of 62 V and 170 nA. Notably, this device was integrated into a fire alarm system, showcasing its potential in real-time fire hazard detection and contributing to public safety applications [29].

In our study, we developed a TENG using butter paper and polyurethane (PU) foam as tribolayers and operated in single-electrode mode. The device achieved a voltage and current of 21 V and 47 nA, respectively. The maximum power of the device was calculated to be 438 nW at  $500 \text{ M}\Omega$ . The device demonstrates stable performance over three weeks, reliable capacitor charging across varying capacitances, and sensitivity to different biomechanical stimuli such as finger, palm, and foot tapping. The integration of the TENG with a neural network classifier enables high-accuracy recognition of input patterns, under-

Department of Electronics and Communication Engineering, Siksha O Anusandhan (deemed to be University), Bhubaneswar 751030, India

<sup>&</sup>lt;sup>2</sup> Department of Electrical Engineering, Siksha O Anusandhan (deemed to be University), Bhubaneswar 751030, India

<sup>&</sup>lt;sup>3</sup> Department of Environmental Sciences, Sambalpur University, Burla 768019, India

<sup>&</sup>lt;sup>4</sup>Department of Physics, Vellore Institute of Technology, Vijayawada 522237, India

<sup>\*</sup>Corresponding author e-mail: ruthvik 015@dgist.ac.kr, basantapanigrahi@soa.ac.in

2 PANDA, A., et al.

scoring its potential for wearable electronics. Furthermore, this study demonstrates a direct mitigation of carbon emissions by transforming routine laboratory waste. Repurposing these otherwise single-use, disposable materials into functional energy devices curbs the volume of non-degradable waste subjected to incineration or landfill, which are notable contributors to greenhouse gas emissions. The process exemplifies circular economy principles, as it diverts waste back into the production cycle, reduces reliance on raw material extraction, and extends material utility.

## 2. Materials and methods

## 2.1 Materials

Several laboratories discarded materials, such as PU foam, butter paper, aluminium tape, and copper wire, are collected and cut into the required size to construct the TENG.

## 2.2 TENG fabrication method

A single-electrode mode TENG was constructed using butter paper as the active triboelectric material (B-TENG), while PU foam was employed as the free-moving layer. Aluminum tape served as the electrode in the device. The active area of the TENG measured  $4~\rm cm \times 4~cm$ . To ensure a stable electrical connection, a copper wire was affixed to the aluminum tape electrode, and the butter paper was securely attached to the electrode surface to maintain device integrity during operation.

## 2.3 Characterisation techniques

The electrical output signals from the TENG were measured using a Keithley 6514 electrometer with LabVIEW software. Mechanical force was applied to the device through a LINMOT linear motor (USA) to ensure consistent and controlled actuation during testing. Surface morphology of tribolayers were analyzed using a scanning electron microscope (SEM) (Hitachi SU-8230, Japan).

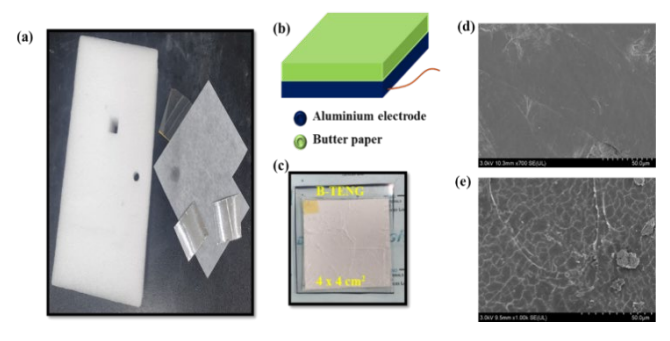
# 3. Results and discussion

Figure 1(a) shows the digital images of the collected discarded items such as PU foam, butter paper, and aluminium tape. Figure 1(b) shows the schematic illustration of B-TENG with layers where aluminium tape serves as the electrode and BP is the active layer. Figure 1(c) shows the digital image of B-TENG. The SEM images of both materials are shown in Figure 1(d-e).

Figure 2 shows the working mechanism of B-TENG, where butter paper as the positive triboelectric layer and PU foam as the negative layer. When the PU foam comes into contact with the butter paper (Figure 2(a)), electrons are transferred from the butter paper to the PU foam due to their differing affinities for electrons, resulting in the butter paper acquiring a net positive charge and the PU foam a net negative charge. Upon separation (Figure 2(b)), this charge imbalance creates a potential difference between the aluminum electrode and the ground. As the PU foam moves away (Figure 2(c)), electrons flow

from the ground to the electrode to balance the potential, generating a current. When the PU foam approaches and contacts the butter paper again (Figure 2(d)), the process reverses, and electrons flow back, producing an alternating current output. This cyclic process of contact and separation leads to the generation of alternating current. SE mode offers greater versatility and device integration, as only one active electrode needs electrical connection while the other can interact freely with the environment. This simplifies device design, enables easy miniaturization, and makes it especially suitable for energy harvesting.

Figure 3 represents the electrical response of B-TENG. The voltage and current output from B-TENG were 21 V and 47 nA, respectively (see Figure 3(a-b)). The Q-t plot of B-TENG is shown in Figure 3(c), and the charge generation is 2nC. The voltage response of B-TENG was measured at various load resistances and is shown in Figure 3(d), which follows the ohmic condition (V = IR, where V = voltage, I = voltage) current, and R = resistance). The maximum power of B-TENG is calculated by using the formula ( $P = V^2/R$ ). B-TENG achieved a maximum power of 438 nW corresponding to 500 M $\Omega$  (see Figure 3(e)). The stability of the B-TENG was systematically monitored over three weeks. As shown in Figure 3(f), the voltage remains same throughout Week 1, Week 2, and Week 3, with no significant degradation in performance. This sustained voltage response indicates excellent durability and stable output characteristics of the B-TENG, confirming its potential for long-term energy harvesting applications. Various capacitors such as 1  $\mu F$ , 2.2  $\mu F$ , 4.7  $\mu F$ , and 10  $\mu F$  were charged for 60 s using B-TENG, as shown in Figure 4(a). Capacitors with lower capacitance values charge more rapidly and reach higher voltages within the given time frame. This trend is attributed to the inverse relationship between capacitance and voltage during charging, where smaller capacitors accumulate voltage faster for a given amount of transferred charge. Figure 4(b) depicts that the stored charge in the capacitor is evaluated by using the expression Q = CV, where Q = charge, C = capacitance, and V = voltage. The B-TENG was able to light up a commercial LED and showcase it as a promising energy harvester, as shown in Figure 4(c). Figure 4(d-f) illustrates the realtime electrical response of the B-TENG under varying mechanical forces induced by finger, palm, and foot tapping. The voltage output increases significantly with the intensity of the applied force, ranging from around 0.4.5 V for finger tapping to above 7.5 V for foot tapping. It demonstrates the device's sensitivity and adaptability to diverse mechanical stimuli, indicating its suitability for wearable and biomechanical energy harvesting systems.



**Figure 1:** (a) Collection of laboratory waste, (b) schematic illustration of B-TENG, (c) digital image of B-TENG, SEM images of (d) butter paper, and (e) PU foam.

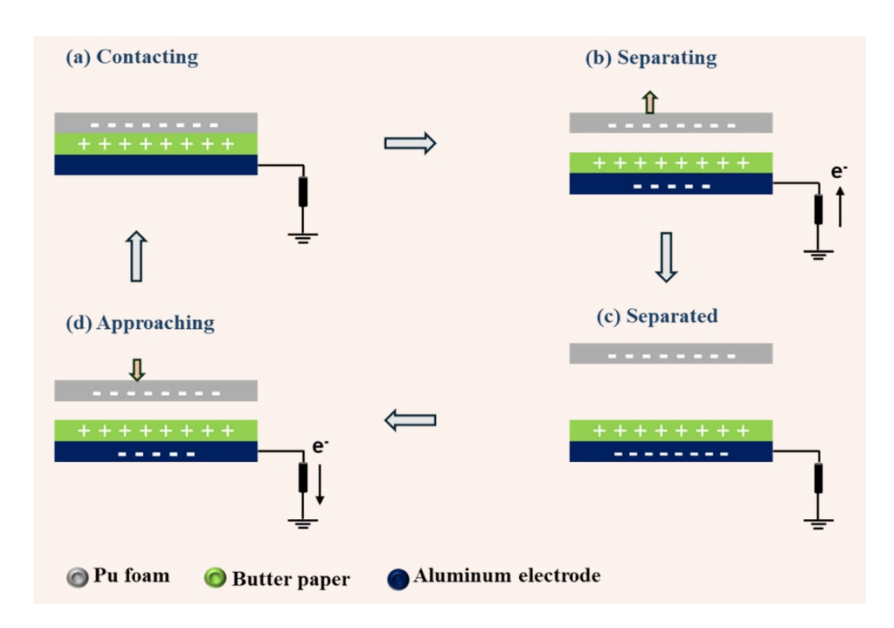


Figure 2. Working mechanism of B-TENG.

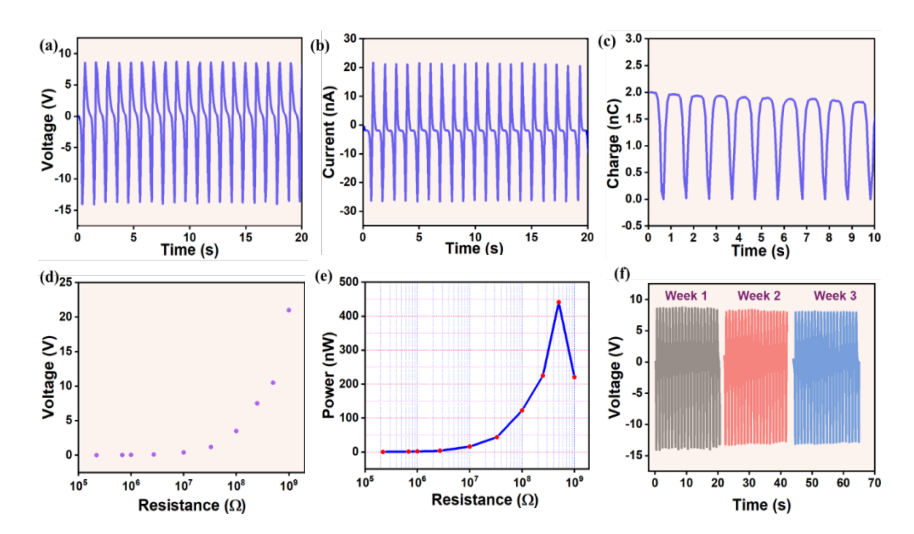


Figure 3: Electrical response of B-TENG (a) voltage, (b) current, (c) charge, (d) voltage across various resistances, (e) calculated power of B-TENG, and (f) week stability of B-TENG.

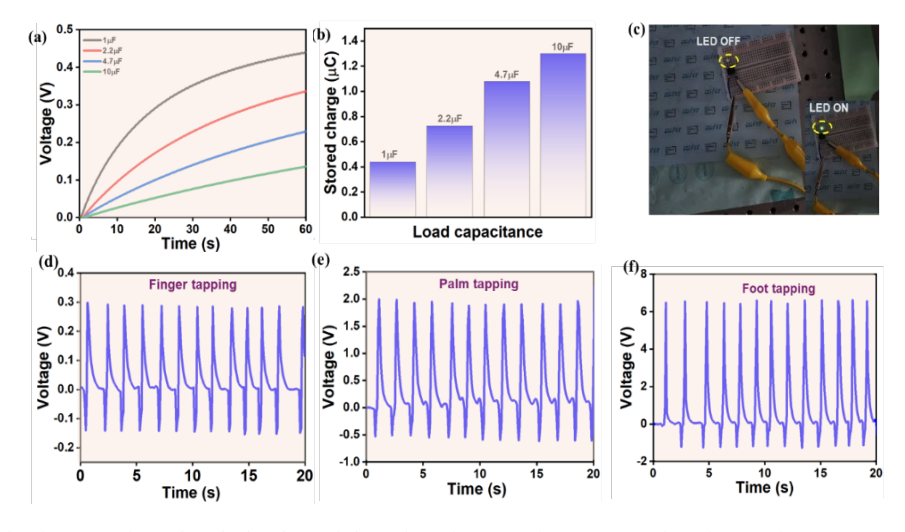


Figure 4. (a) Charging of various capacitors, (b) calculated stored charge in various capacitors, (c) powering of LED using B-TENG, and (d-f) electrical response of B-TENG using different mechanical motions.

4 PANDA, A., et al.

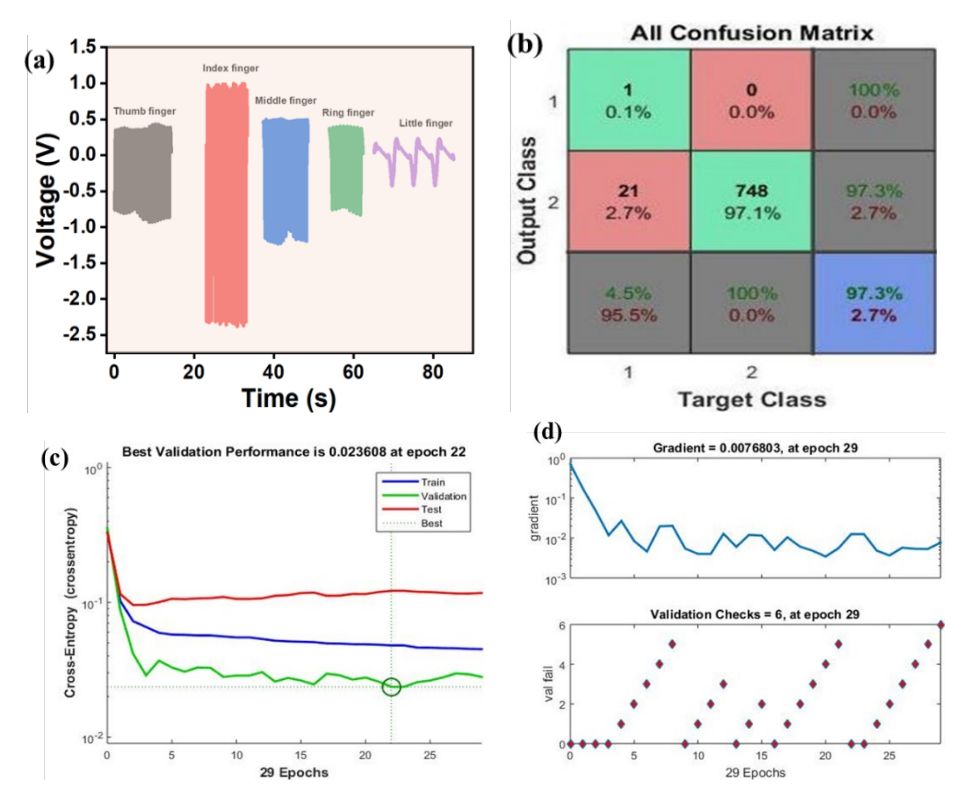


Figure 5. (a) Voltage response of B-TENG from different fingers, (b) confusion plot of the combined neural network, (c) the best validation performance of the network, and (d) gradient and validation checks.

Table 1. Comparison table of our study with state of art of other TENGs.

Tribolayer 1	Tribolayer 2	Voltage	Current	Reference
Waste textile	FEP	19 V	8 μΑ	[27]
Cigarette filters	Plastic waste	42.8 V	0.86 μΑ	[28]
Cotton fabric	Kapton	62 V	170 nA	[29]
Butter paper	PU foam	21 V	47 nA	This work

Figure 5(a) shows the ability of B-TENG to convert biomechanical motions from different fingers into measurable electrical signals. The varying outputs reflect differences in finger size and movement dynamics. This characteristic can be utilized in wearable electronics, gesture recognition systems, and self-powered human-machine interfaces. To generate the relevant data sets, this model makes use of the acceleration of the various finger taps. Artificial neural networks (ANN) are often considered more flexible and advantageous than other techniques due to their unique strength towards nonlinear problem solving. ANN can automatically learn nonlinear and complex patterns, which is crucial for interpreting the electrical outputs of TENG generated by finger movement. In complex tasks like irregular voltage signal processing, ANNs outperform traditional machine learning models by a large margin. ANN models can generalize better if trained properly with sufficient data, making them suitable for real-time unpredictable scenarios. Voltage output generated by different finger taps at different times and biomechanical motions is used as a relevant dataset for ANN. When training an ANN, the entire dataset is split into three parts: training, testing, and validation sets and transforming them into one-dimensional arrays. Training uses 70% of the data, testing uses 15%, and validation uses 15%. Here, a total of 770 voltage samples is taken, out of which 540 samples are used for training the network. Each of the 115 samples is used for testing and validation of the network. The training set teaches the ANN to recognize patterns (e.g., voltage for motion/gesture). The validation set ensures the model generalizes, not memorizes. The testing set shows how well the model will work on real-world, unseen TENG signals. After computing the hidden layer and using the feature parameters of various structures as input, the output layer displays the prediction results. We selected pre-existing experimental data as datasets and separated them into training, validation, and test sets in order to confirm the simulation's accuracy. The classification accuracy of the neural network is shown in the confusion matrix in Figure 5(b). The diagonal cells show the datasets that have been correctly classified, whereas the off-diagonal cells show the datasets that have been wrongly classified. The total percentage of cases that were correctly classified in green and those that were mistakenly classified in red is shown in the blue cell on the bottom right. During testing, 97.3% (749 out of 770) were correctly classified, while 2.7% (21 out of 770) were wrongly classified, according to the total confusion matrix. The training set data is used to train the model. The model can also be validated by the forced stop approach using the validation set data as a criterion. The neural network model consists of two output layers, ten hidden layers, and five input layers. Figure 5(c) describes the network's optimal validation performance

as shown by performance graphs. The validation's efficacy is 0.023608. The optimal value for the validation phase is identified after 22 epochs. The gradient and validation check graphs are displayed. The gradient value after 29 epochs is 0.0076803. The gradient and validation check for the suggested neural network model are displayed in Figure 5(d). Table 1, presents a comparative analysis of relevant studies to contextualize our work.

## 4. Conclusion

This study demonstrates the potential of upcycling commonly discarded laboratory materials, specifically butter paper and polyurethane foam, into functional TENGs. The fabricated device, operating in a single-electrode mode, consistently produced notable electrical output of 21 V, 47 nA, with excellent stability sustained over several weeks. Its capability to charge capacitors efficiently and illuminate LEDs exemplifies its utility as a reliable energy harvester for low-power applications. Furthermore, the integration of B-TENG signals with a neural network model highlights its suitability for gesture recognition and human—machine interfaces. The device's robust performance, durability, and adaptability to diverse stimuli underscore its promising role in sustainable energy harvesting and smart sensing platforms. By merging waste valorisation with advanced energy technologies, this approach offers a scalable pathway towards resource-efficient, environmentally responsible scientific practice.

## References

- [1] A. Villanueva, and H. Wenzel, "Paper waste–recycling, incineration or landfilling? A review of existing life cycle assessments," *Waste management*, vol. 27, no. 8, pp. S29-S46, 2007.
- [2] K. Pivnenko, E. Eriksson, and T. F. Astrup, "Waste paper for recycling: Overview and identification of potentially critical substances," *Waste management*, vol. 45, pp. 134-142, 2015.
- [3] S. A. Behera, S. Panda, S. Hajra, K. R. Kaja, A. K. Pandey, A. Barranco, S. M. Jeong, V. Vivekananthan, H. J. Kim, and P. G. R. Achary, "Current trends on advancement in smart textile device engineering," *Advanced Sustainable Systems*, vol. 8, no. 12, p. 2400344, 2024.
- [4] M. C. Monte, E. Fuente, A. Blanco, and C. Negro, "Waste management from pulp and paper production in the European Union," *Waste management*, vol. 29, no. 1, pp. 293-308, 2009.
- [5] A. Panda, K. K. Das, K. R. Kaja, M. Belal, and B. K. Panigrahi, "Single electrode mode triboelectric nanogenerator for recognition of animal sounds," *Journal of Metals, Materials and Minerals*, vol. 34, no. 4, pp. 2170-2170, 2024.
- [6] B. Ahmadi, and W. Al-Khaja, "Utilization of paper waste sludge in the building construction industry," *Resources, conservation and recycling*, vol. 32, no. 2, pp. 105-113, 2001.
- [7] K. U. Kumar, S. Hajra, G. M. Rani, S. Panda, R. Umapathi, S. Venkateswarlu, H. J. Kim, Y. K. Mishra, and R. R. Kumar, "Revolutionizing waste-to-energy: harnessing the power of triboelectric nanogenerators," *Advanced Composites and Hybrid Materials*, vol. 7, no. 3, p. 91, 2024.

- [8] Y. Zi, J. Wang, S. Wang, S. Li, Z. Wen, H. Guo, and Z. L. Wang, "Effective energy storage from a triboelectric nanogenerator," *Nature communications*, vol. 7, no. 1, p. 10987, 2016.
- [9] G. Zhu, B. Peng, J. Chen, Q. Jing, and Z. L. Wang, "Triboelectric nanogenerators as a new energy technology: From fundamentals, devices, to applications," *Nano Energy*, vol. 14, pp. 126-138, 2015.
- [10] K. R. Kaja, S. A. Behera, B. Das, S. Hajra, S. Panda, M. A. Belal, N. Vittayakorn, B. Nanda, P. G. R. Achary, and H. J. Kim, "Calcium copper titanate particles based energy harvesting and removal of pharmaceutical pollutants," ACS Applied Electronic Materials, vol. 7, no. 9, pp. 4327-4338, 2025.
- [11] R. Dharmasena, and S. Silva, "Towards optimized triboelectric nanogenerators," *Nano Energy*, vol. 62, pp. 530-549, 2019.
- [12] B. Mahale, N. Kumar, R. Pandey, and R. Ranjan, "High power density low-lead-piezoceramic-polymer composite energy harvester," *IEEE Transactions on Ultrasonics, Ferroelectrics,* and Frequency Control, vol. 66, no. 4, pp. 789-796, 2019.
- [13] S. Niu, and Z. L. Wang, "Theoretical systems of triboelectric nanogenerators," *Nano Energy*, vol. 14, pp. 161-192, 2015.
- [14] W.-G. Kim, D.-W. Kim, I.-W. Tcho, J.-K. Kim, M.-S. Kim, and Y.-K. Choi, "Triboelectric nanogenerator: Structure, mechanism, and applications," ACS nano, vol. 15, no. 1, pp. 258-287, 2021.
- [15] Y. Wang, Y. Yang, and Z. L. Wang, "Triboelectric nanogenerators as flexible power sources," *npj Flexible Electronics*, vol. 1, no. 1, p. 10, 2017.
- [16] S. Mishra, M. Rakshita, H. Divi, S. Potu, and R. K. Rajaboina, "Unique contact point modification technique for boosting the performance of a triboelectric nanogenerator and its application in road safety sensing and detection," ACS Applied Materials & Interfaces, vol. 15, no. 27, pp. 33095-33108, 2023.
- [17] J. A. L. Jayarathna, and K. R. Kaja, "Energy-harvesting device based on lead-free perovskite," *AI, Computer Science and Robotics Technology*, 2024.
- [18] K. R. Kaja, S. Hajra, S. Panda, M. A. Belal, P. Pakawanit, N. Vittayakorn, C. R. Bowen, H. Khanbareh, and H. J. Kim, "Triboelectrification based on the waste waterproof textiles for multisource energy harvesting," *Advanced Sustainable Systems*, vol. 9, no. 5, p. 2400678, 2025.
- [19] M. Rakshita, M. Navaneeh, A A. Sharma, P. P. Pradhan, K. A. K. D. Prasad, U. K. Khanapuram, R. R. Kumar, and H. Divi, "Phosphor-Based triboelectric nanogenerators for mechanical energy harvesting and self-powered systems," *ACS Applied Electronic Materials*, vol. 6, no. 3, pp. 1821-1828, 2024.
- [20] P. Gajula, B. Mahanty, and D.-W. Lee, "Engineered nano-micro fiber networks: PANI nanowires on electrospun Nylon 11 fibers for enhanced triboelectric performance in wearable biomechanical sensing," *Materials Today Nano*, vol. 29, p. 100602, 2025.
- [21] H.-S. Kim, N. Kumar, J.-J. Choi, W.-H. Yoon, S. N. Yi, and J. Jang, "Self-powered smart proximity-detection system based on a hybrid magneto-mechano-electric generator," *Advanced Intelligent Systems*, vol. 6, no. 1, p. 2300474, 2024.
- [22] D. Zawar, S. Mishra, R. Muddamalla, P. P. Pradhan, K. A. K. D. Prasad, S. Potu, M. Navaneeth, J. Pani, N. K. Babu, H. Borkar, R. R. Kumar, and D. Haranath, "Synergistic optimization of europium-doped yttria for photoluminescence and triboelectric

6 PANDA, A., et al.

nanogenerator applications," *Energy Technology*, vol. 12, no. 7, p. 2400573, 2024.

- [23] P. Gajula, J. U. Yoon, I. Woo, and J. W. Bae, "Harnessing mechanical energy for green hydrogen: pioneering highperformance triboelectric nanogenerators," *Advanced Functional Materials*, p. 2501074, 2025.
- [24] S. Hajra, V. Vivekananthan, M. Sahu, G. Khandelwal, N. P. M. J. Raj, and S.-J. Kim, "Triboelectric nanogenerator using multiferroic materials: An approach for energy harvesting and self-powered magnetic field detection," *Nano Energy*, vol. 85, p. 105964, 2021.
- [25] S. Panda, S. Hajra, H. Kim, J. Seo, B. Jeong, I. Lee, K. R. Kaja, M. A. Belal, V. Vivekananthan, H. Khanbareh, C. R. Bowen, K. Mistewicz, and H. J. Kim, "An overview of flame-retardant materials for triboelectric nanogenerators and future applications," Advanced Materials, vol. 37, no. 9, p. 2415099, 2025.

- [26] M. Rakshita, A. Babu, K. Jayanthi, S. Bathula, K. U. Kumar, and D. Haranath, "Studies on contact angle measurements in superoleophobic aluminum hydroxide nanoflakes," *Materials Letters*, vol. 315, p. 131938, 2022.
- [27] S. Hajra, K. R. Kaja, S. Panda, M. A. Belal, B. K. Panigrahi, P. Pakawanit, and H. J. Kim, "Waste based triboelectric nanogenerator for energy harvesting and self-powered sensors," *Journal of Cleaner Production*, p. 145591, 2025.
- [28] G. M. Rani, C.-M. Wu, K. G. Motora, and R. Umapathi, "Waste-to-energy: Utilization of recycled waste materials to fabricate triboelectric nanogenerator for mechanical energy harvesting," *Journal of Cleaner Production*, vol. 363, p. 132532, 2022.
- [29] B. Jeong, J. Seo, S. Panda, S. Hajra, H. Kim, I. Lee, K. R. Kaja, M. A. Belal, D. P. Dubal, and H. J. Kim, "Chitosan-phytic acidbased flame-retardant triboelectric nanogenerator for fire safety applications," *Advanced Sustainable Systems*, p. e00212, 2025.